

The Added Value of Apparent Diffusion Coefficient Measurement in the Evaluation of Hepatocellular Carcinoma after Locoregional Therapy Utilizing LI-RADS Treatment Response Algorithm

FATMAELZAHRAA A. DENEWAR, M.D.¹; BASMA A. ELGED, M.D.¹; EL SHIMAA S. ELERAKY, M.D.²; REHAM ALGHANDOUR, M.D.³; GEHAD A. SALEH, M.D.¹ and MARWA SALEH, M.D.⁴

The Department of Diagnostic Radiology, Faculty of Medicine, Mansoura University¹, Department of Internal Medicine, Faculty of Medicine, Horus University², Department of Medical Oncology, Oncology Center, Mansoura University³ and Department of Internal Medicine, Faculty of Medicine, Mansoura University⁴

Abstract

Background: To evaluate the additional utility of apparent diffusion coefficient measurement to the treatment response algorithm of the Liver Imaging Reporting and Data System version 2018.

Aim of Study: For the purpose of assessing therapeutic response following locoregional hepatocellular carcinoma treatment.

Material and Methods: 110 patients with previously treated HCC who underwent liver magnetic resonance imaging (MRI) were included in this retrospective analysis. According to the LR-TR grading system, treated hepatocellular carcinomas were divided into 3 groups: LR-TR nonviable, LR-TR equivocal, and LR-TR viable. Two blinded reviewers independently determined the ADCmean measures of the treated lesions.

Results: According to both observers, the ADC mean values for viable HCC were 1.04 ± 0.18 and $1.026 \pm 0.17 \times 10^{-3} \text{mm}^2/\text{s}$, non-viable HCC was 1.48 ± 0.19 and $1.47 \pm 0.19 \times 10^{-3} \text{mm}^2/\text{s}$, and equivocal HCC was 1.29 ± 0.18 and $1.29 \pm 0.18 \times 10^{-3} \text{mm}^2/\text{s}$. With respect to viable HCC ($r=0.93$), non-viable HCC ($r=0.805$), and equivocal HCC ($r=0.98$), there was great similarity between the two assessments. Both observers utilized the same ADC mean cut-off value of 1.355 and $1.251 \times 10^{-3} \text{mm}^2/\text{s}$ with (AUC) of 0.8 and 0.92 to distinguish between viable and non-viable HCC. With an AUC of 0.853 and 0.87, the ADC mean cut-off values utilized to distinguish between viable and equivocal HCC were 1.206 and $1.1125 \times 10^{-3} \text{mm}^2/\text{s}$, respectively. With AUC values of 0.82 and 0.76, the ADC mean cut-off values utilized to distinguish between non-viable and equivocal HCC were 1.426 and $1.372 \times 10^{-3} \text{mm}^2/\text{s}$, respectively.

Conclusions: The LI-RADS-v2018 TR algorithm may perform better and be used in clinical settings if ADC measurement is included.

Correspondence to: Dr. Basma A. Elged,
E-Mail: basmaelged@mans.edu.eg

Key Words: Hepatocellular carcinoma – MR-Imaging – MR-Diffusion – Ablation procedures – Liver – Chemoembolization.

Introduction

DUE to a variety of factors, including multifocality, impaired liver function, vascular infiltration, and extrahepatic tumor symptoms, the majority of hepatocellular carcinoma diagnosed patients are unable to undergo immediate curative resection [1,2].

For patients who are ineligible for surgery or who need to be down staged before a liver transplant, locoregional therapy (LRT) of HCC, which includes transarterial chemoembolization (TACE) and local ablative therapy like radiofrequency ablation (RFA) or microwave ablation (MWA), is frequently used [2-6].

List of Abbreviations:

HCC	: Hepatocellular carcinoma.
LRT	: Locoregional therapy.
TACE	: Transarterial chemoembolization.
RFA	: Radiofrequency ablation.
MWA	: Microwave ablation.
CT	: Computed tomography.
MRI	: Magnetic resonance imaging.
DWI	: Diffusion-weighted imaging.
ADC	: Apparent diffusion coefficient.
LI-RADS	: Liver Imaging Reporting and Data System.
LR-TR	: LI-RADS treatment response.
mRECIST	: Modified Response Evaluation Criteria in Solid Tumors.
EASL	: European Association for the Study of the Liver.
APHE	: Arterial phase hyperenhancement.
AUC	: Area under the curve.
PI-RADS	: Prostate Imaging Reporting and Data System.
O-RADS	: Ovarian-adnexal reporting and data system.

Evaluation of treatment response is essential for patient follow-up and future treatment decisions after LRT for HCC [7,8]. Major worldwide guidelines suggested dynamic contrast-enhanced computed tomography or (MRI) for the early diagnosis of residual or local tumor recurrence [5,6].

However, dynamic contrast enhanced MRI is still unable to distinguish between residual tumor and post-therapeutic inflammatory effects [6-9]. The development of diffusion-weighted imaging (DWI) made it easier to find both necrotic and remaining tissue [10]. Due to its significant inverse association with the degree of cellularity, apparent diffusion coefficient (ADC) enables quantitative evaluation of the diffusion magnitude of water molecules inside the interstitial space [11,12].

Following the requirement for a systematized method of image interpretation and reporting after LRT, the Liver Imaging Reporting and Data System (LI-RADS) created a treatment response algorithm in 2017 [7]. With the aid of post-treatment imaging features on contrast-enhanced CT or MRI scans, the LI-RADS treatment response (LR-TR) algorithm classified treated observations as either LR-TR viable (probably or certainly viable), LR-TR equivocal (equivocally viable), or LR-TR nonviable [7].

Additionally, according to the modified Response Evaluation Criteria in Solid Tumours (mRECIST) and European Association for the Study of the Liver (EASL) criteria [7-9], arterial phase hyperenhancement (APHE) was the only feature of a viable tumour. However, the LR-TR algorithm added new imaging features for the viability of HCC, including appearance washing out and enhancement similar to pretreatment. This algorithm was validated by several studies [13-15]. The current LI-RADS treatment response algorithm bases its assessment of tumor activity mostly on APHE and washout features, while T2 hyperintensity and diffusion limitation are viewed as supplementary findings [7]. ADC is not, however, a part of this method. Therefore, the purpose of this study is for determination whether adding ADC measurement to LR-TR algorithm.

Material and Methods

Patient and inclusion criteria:

Because the institutional review board approved this retrospective inquiry, informed consent was not necessary. From March 2021 to May 2022, 117 HCC patients who received either local ablative treatment or TACE were chosen. Patients who received contrast-enhanced dynamic MR imaging and liver DWI 4 to 6 weeks following locoregional treatment met the inclusion criteria. We excluded 7 patients from the research because respiratory motion artefact reduced the picture quality, and we classified them as LR-TR non-evaluable (treated response not evaluable). The final cohort consequently included 110 individuals (92 men and 18 women) with a mean

age of 54 years (49-61 yrs) and 126 HCC lesions. The 126 HCC lesions that were included received either RFA (38/126; 30.2 percent), MWA (36/126; 28.6%), or TACE utilizing lipiodol as an embolic agent (52/126; 41.2%).

MR imaging technique:

Dynamic contrast-enhanced and DWI MR exams were carried out on all patients at baseline and 4-6 wks following the first loco-regional therapy using a 1.5 Tesla scanner (Ingenia®, Philips Healthcare). T1-weighted imaging without contrast and T2-weighted imaging were obtained. Multiphase postcontrast T1-weighted GRE sequence with the following acquisition settings: TR/TE 3.3-4.5/1.4-1.9ms, flip angle 10°, number of excitations (NEX) 2, matrix size 172x135, field of view 300-400mm, and slice thickness of 3-5mm after gadolinium injection (0.5mmol/mL at a dose of 0.2mL/kg of body). DWI was performed as single-shot echo-planar imaging using *b*-values of 0,100, 600 and 1000 s/mm². ADC maps were generated using a mono exponential fit of the acquired *b*-value data points. DWI acquisition parameters were as the following: TR/TE=1900-70ms, NEX=3, matrix=124 x 120, slice thickness=5mm, slice gap=1-2mm and scan time=70sec. Images were moved to a separate workstation (Phillips Advantage windows workstation) that was outfitted with a commercially available post-processing tool.

MR imaging analysis:

Two radiologists (GAS and BAE) with 8 and 12 years of expertise in abdominal imaging, respectively, independently evaluated each MR image.

The classification of patients and evaluation of therapy response both utilised the LR-TR method [15,16]. Patients were thus divided into the following three major categories (after excluding lesions that could not be evaluated due to poor picture quality):

- 1- LR-TR nonviable lesions are those that are “probably or definitely nonviable” in the absence of pathological enhancement or if enhancement is anticipated at the site of treatment. This category also includes lesions that are not apparent after treatment or don’t have any LR-TR viable traits.
- 2- LR-TR equivocal lesions that are “equivocally viable”: If the enhancement pattern doesn’t meet the criteria for being likely benign or unquestionably viable.
- 3- LR-TR viable lesions “probably or definitely viable”: If the treated lesion has nodules, masses, or irregular thick tissue, as well as arterial enhancement or washout and/or enhancement that is comparable to that which existed prior to embolisation. The treatment response approach still does not take ancillary characteristics supporting malignancy, such as T2 hyperintensity and restricted diffusion, into account.

To make sure that each reviewer evaluated the same lesion in instances with numerous observations, each HCC was individually analysed and reported by its size as well as its segmental location.

ADC maps were connected with T1WI, T2WI, and contrast enhanced T1WI for quantitative assessment and ADC mean measurement, avoiding areas of haemorrhage and necrosis, as well as artefacts from chemical shift and magnetic susceptibility. Additionally, the lesion’s rim was not included, particularly after RFA or MWA. In order to compute the ADC, three circular regions of interest (ROIs) of 10mm² each were established over the suspected malignancy in viable and equivocal lesions, as well as over the whole ablation zones in nonviable lesions. The ADC mean values were then averaged.

Reference standard:

The dynamic MRI characteristics in accordance with LI-RADS treatment response v2018 were used as the reference standard [7].

Lesions classified as LR-TR viable or equivocal were scheduled for retreatment, while follow-up was taken into account for nonviable and equivocal lesions. In our facility, tissue biopsy and pathological confirmation were not frequently performed due to the technical complexity and patient resistance.

Statistical analysis:

The ADC value’s mean and standard deviation were computed. With the Mann-Whitney test, continuous parametric variables were compared. A substantial difference was deemed to exist when $p < 0.05$ was used.

To gauge this, the intraclass correlation coefficient (ICC) was determined. Interrater reliability: Values below 0.5, below 0.75, between 0.75 and 0.9, above 0.9 indicate low moderate, good and outstanding reliability respectively [17].

The area under the curve (AUC) for the ADC of the 3 different categories of LI-RADS TR algorithm was computed after performing a receiver operating characteristic study. The SPSS programme was used to conduct all statistical analyses.

Results

Each observer examined 126 treated HCCs altogether. The number of liver observations made by each of the two observers within each LR-TR category is shown in (Table 1). However, the examination of ADC measurements in the two observers assessments of various LR-TR categories was the main emphasis of this investigation.

According to both observers’ respective mean ADC values, viable HCC was 1.04 ± 0.18 and $1.026 \pm 0.17 \times 10^{-3} \text{mm}^2/\text{s}$, non-viable HCC was 1.48 ± 0.19 and $1.47 \pm 0.19 \times 10^{-3} \text{mm}^2/\text{s}$, and equivocal HCC was 1.29 ± 0.18 and $1.29 \pm 0.18 \times 10^{-3} \text{mm}^2/\text{s}$ (Figs. 1-3). With a $p < 0.0001$, it was found that the mean ADC of viable HCC was considerably lower than that of non-viable HCC in both studies. Between the TACE, RFA, and MWA-Groups, there were no appreciable variations in the ADC values within the lesion.

Both assessments for viable HCC and equivocal HCC had very high interrater reliability ($r = 0.93$ and $r = 0.98$). Non-viable HCC showed good interobserver reliability ($r = 0.805$). (Table 2).

Both observers employed cutoff ADC values of < 1.355 and $< 1.251 \times 10^{-3} \text{mm}^2/\text{s}$ with (AUC) of 0.8 and 0.92 to distinguish between viable and non-viable HCC. With an AUC of 0.853 and 0.87, the cutoff ADC utilized to distinguish between viable and equivocal HCC was < 1.206 and $< 1.1125 \times 10^{-3} \text{mm}^2/\text{s}$. With an AUC of 0.82 and 0.76, the cutoff ADC utilized to distinguish between non-viable and equivocal HCC was < 1.426 and $< 1.372 \times 10^{-3} \text{mm}^2/\text{s}$, respectively (Figs. 4-6). (Table 3).

Table (1): Observations number made by each observer in each LI-RADS category.

	Observer 1 N=126 (%)	Observer 2 N=126 (%)
Viable	27 (21.4%)	30 (23.8%)
Non-viable	96 (76.2%)	92 (73%)
Equivocal	3 (2.4%)	4 (3.2%)

Table (2): Intraclass correlation coefficient (ICC) categorize ADC ($\times 10^{-3} \text{mm}^2/\text{s}$) of LI-RADS treatment response (LR-TR).

	Ob 1	Ob 2	ICC
ADC viable	1.04 ± 0.18 (0.85-1.6)	1.026 ± 0.17 (0.84-1.59)	$r = 0.93$ $p < 0.001^*$
ADC non-viable	1.48 ± 0.19 (0.91-1.82)	1.47 ± 0.19 (0.91-1.8)	$r = 0.805$ $p < 0.001^*$
ADC equivocal	1.29 ± 0.18 (1.01-1.44)	1.31 ± 0.19 (1.22-1.5)	$r = 0.98$ $p = 0.003^*$

Table (3): Results of ROC considering both ADC measurements were utilized to distinguish between viable, non-viable, and equivocal HCC.

	Cutoff	AUC	Sensitivity	Specificity	Accuracy
<i>Viable vs. non-viable:</i>					
1 st observer	1.355	0.89	88.3	93.3	89.72
2 nd observer	1.251	0.92	92.9	90.0	91.59
<i>Viable vs. equivocal:</i>					
1 st observer	1.206	0.853	80.0	86.7	85.7
2 nd observer	1.1125	0.87	80.0	80.0	82.5
<i>Non-viable vs. equivocal:</i>					
1 st observer	1.426	0.82	74.0	80.0	74.4
2 nd observer	1.372	0.76	90.9	60.0	70.5

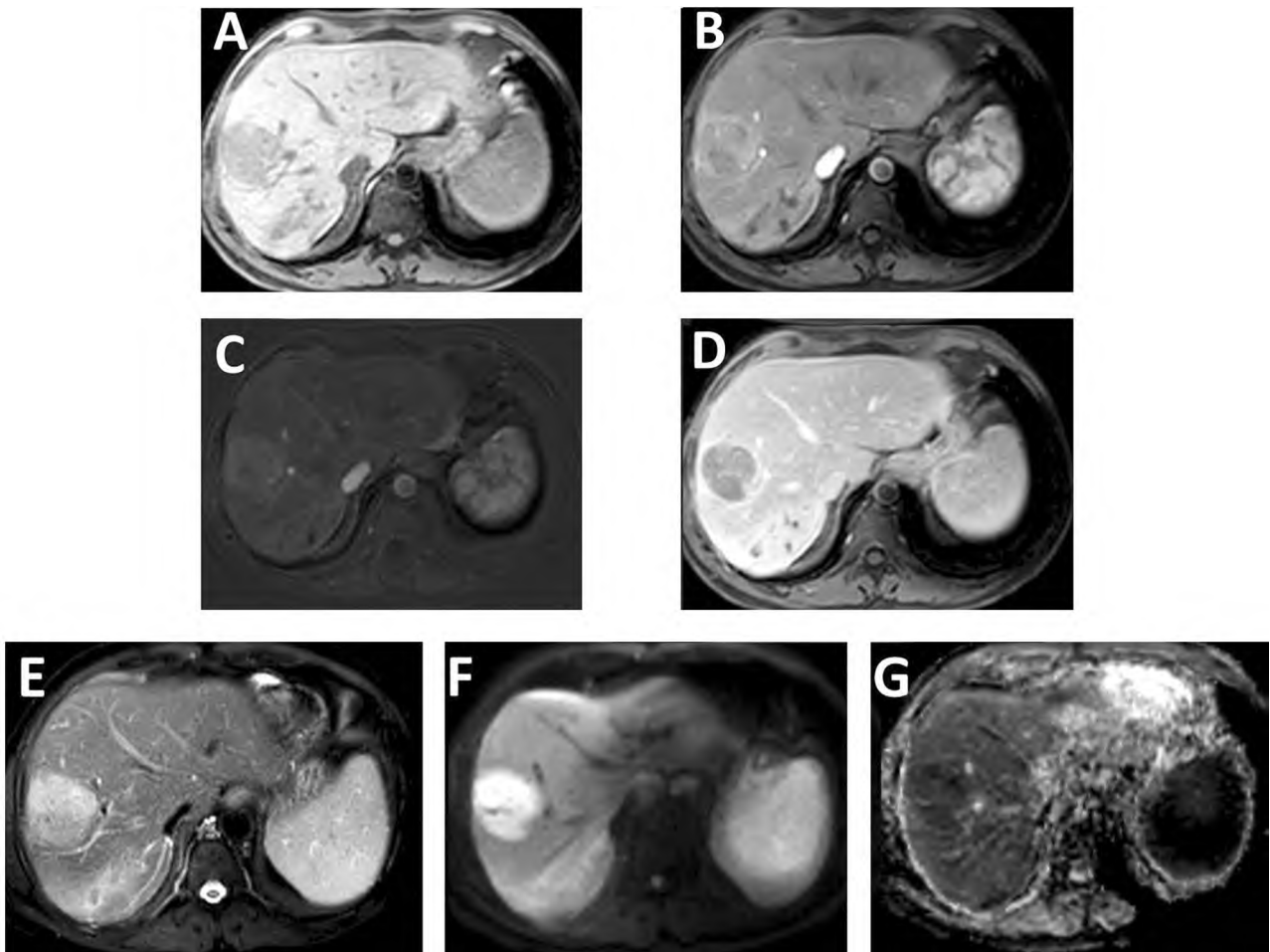


Fig. (1): LR-TR Viable lesion in a 50-year-old man after both RF and TACE.

A- Axial non-contrast T1-WI revealed hypointense lesion in segment VII.

B- Enhanced T1-WI arterial phase revealed diffuse mass-like enhancement of the lesion.

C- Subtracted T1-WI confirmed the enhancement.

D- Enhanced T1-WI delayed phase revealed washout and capsular enhancement.

E- Fat-suppressed T2-WI revealed mild to moderate hyperintensity of the lesion.

F, G- DWI ($b = 800 \text{ s/mm}^2$) and corresponding ADC map revealed restricted diffusion pattern. ADC values by both reviewers were $1.01 \times 10^{-3} \text{ mm}^2/\text{s}$ and $1.05 \times 10^{-3} \text{ mm}^2/\text{s}$ respectively.

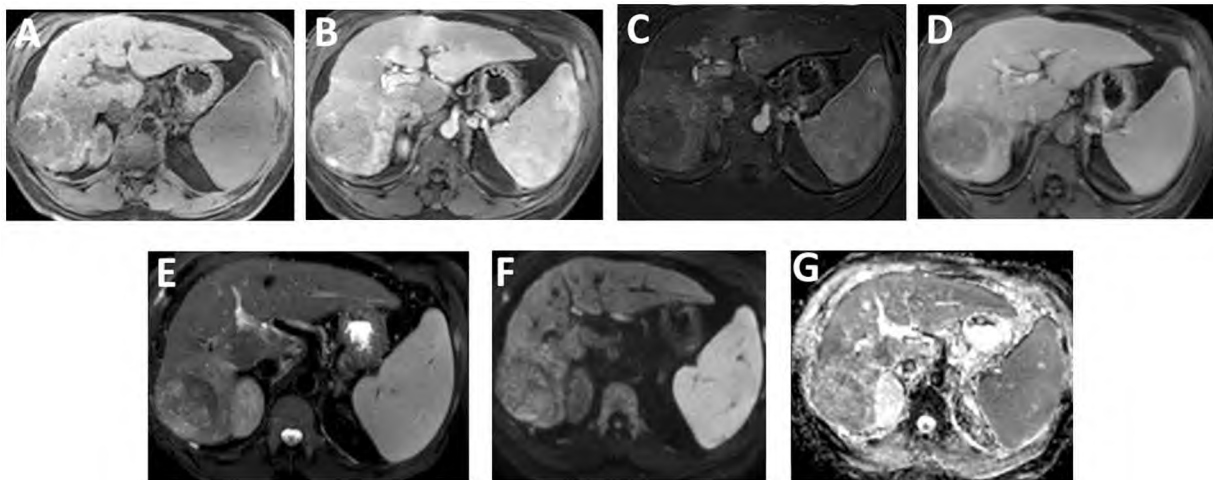


Fig. (2): LR-TR Equivocal lesion in a 55-year-old man after TACE.

- A- Axial non-contrast T1-WI revealed hypointense lesion in segment VII.
- B- Enhanced T1-WI arterial phase revealed irregular thick nodular enhancement of the lesion.
- C- Subtracted T1-WI confirmed the enhancement.
- D- Enhanced T1-WI delayed phase revealed no washout.
- E- Fat-suppressed T2-WI revealed mild to moderate hyperintensity of large part of treated lesion not corresponding to the enhancing part.
- F, G- DWI ($b = 800 \text{ s/mm}^2$) and corresponding ADC map revealed unrestricted diffusion pattern. ADC values by both reviewers were $1.18 \times 10^{-3} \text{ mm}^2/\text{s}$ and $1.21 \times 10^{-3} \text{ mm}^2/\text{s}$ respectively.

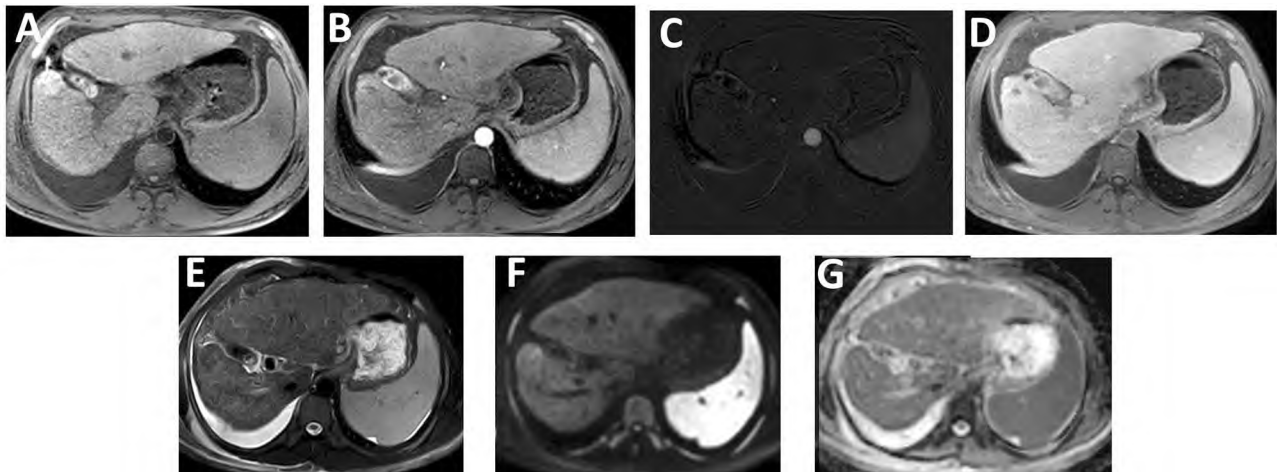


Fig. (3): LR-TR Nonviable lesion in a 47-year-old man after TACE.

- A- Axial non-contrast T1-WI revealed hyperintense lesion in segment V.
- B- Enhanced T1-WI arterial phase revealed no significant enhancement of the lesion.
- C- Subtracted T1-WI confirmed the absence of enhancement.
- D- Enhanced T1-WI delayed phase revealed no washout.
- E- Fat-suppressed T2-WI revealed hypointensity of the lesion.
- F, G- DWI ($b = 800 \text{ s/mm}^2$) and corresponding ADC map revealed unrestricted diffusion pattern. ADC values by both reviewers were $1.31 \times 10^{-3} \text{ mm}^2/\text{s}$ and $1.33 \times 10^{-3} \text{ mm}^2/\text{s}$ respectively.

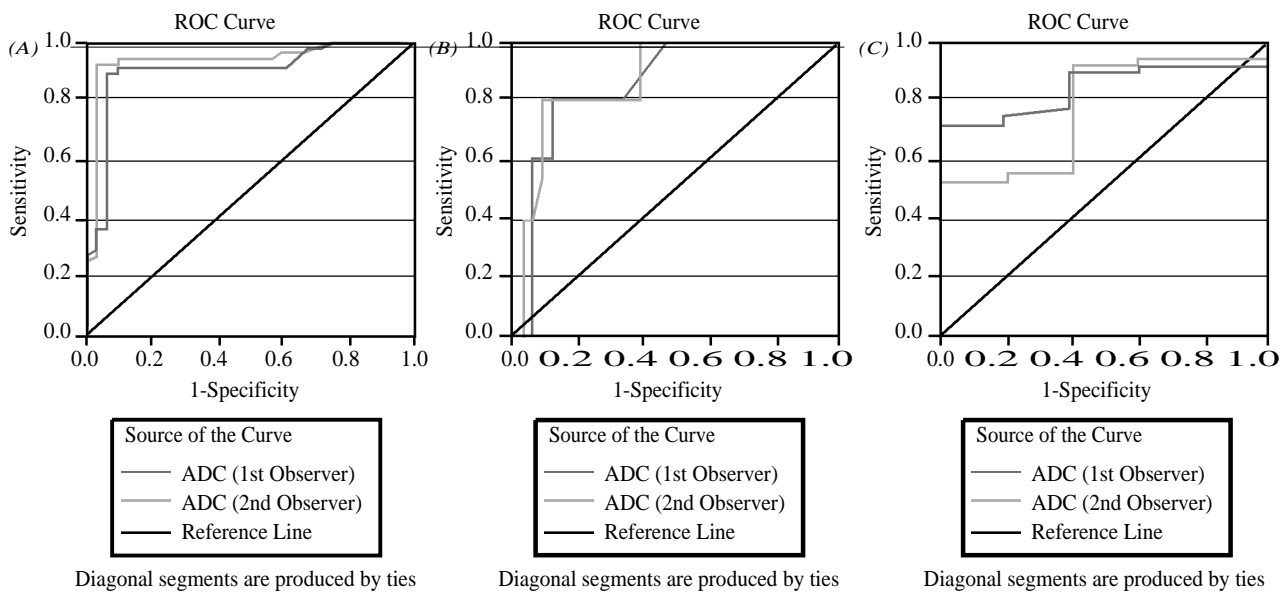


Fig. (4): ROC curve. Cutoff ADC value used to differentiate viable from nonviable HCC (A): Viable from equivocal HCC (B) and nonviable from equivocal HCC by both observers were ≤ 1.35 and $\leq 1.25 \times 10^{-3} \text{ mm}^2/\text{s}$, ≤ 1.2 and $\leq 1.11 \times 10^{-3} \text{ mm}^2/\text{s}$ and ≤ 1.42 and $\leq 1.37 \times 10^{-3} \text{ mm}^2/\text{s}$ with area under curve (AUC) of 0.89 and 0.92, 0.85 and 0.87 and 0.82 and 0.76 respectively.

Discussion

Since it can boost the reader's confidence and standardize the report terms, the LI-RADS TR algorithm is now frequently used for evaluation the therapeutic response of HCC after various treatment procedures. A recent study we conducted on the major imaging features of LI-RADS v2018 indicated high inter-observer agreement for the major imaging features of LR-1, LR-2, LR-5, LR-M, and LR-TIV, as well as good interobserver agreement for LR-3 and LR-4 [14]. So, in the current study we focused only on the ADC analysis.

In this retrospective investigation, we discovered that the ADC values for both readings for viable and equivocal HCC had strong interrater reliability ($r=0.93$ and 0.98 , respectively), with good reliability for non-viable HCC.

According to both reviewers, the ADC mean threshold values for benign tissue changes in non-viable lesions were $1.35 \times 10^{-3} \text{ mm}^2/\text{s}$ and $1.25 \times 10^{-3} \text{ mm}^2/\text{s}$, respectively, and were significantly higher than the ADC mean for recurring or persistent malignant tissue in live lesions. This may be explained by the benign post-ablation alterations, such as edema, hyperemia, and inflammatory changes, having lower cellularity than the malignant lesions [18]. Our findings corroborated those of Mahmoud et al. [19], who discovered that an ADC threshold value of $1.11 \times 10^{-3} \text{ mm}^2/\text{s}$ can be used to distinguish between tumor viability and treatment-related specific benign parenchymal enhancement.

ADC would be a trustworthy indication of tumor response following TACE, according to two recent meta-analyses that tested its usefulness in identify-

ing residual or recurrent HCC after TACE [20,21]. Similar outcomes were observed in previous trials that examined the value of ADC in HCC patients receiving ablative radiation [22,23]. However, these investigations used mRECIST or EASL criteria to standardize the response evaluation.

Prostate imaging reporting and data system (PI-RADS)-v2 was shown to highlight the increased benefit of ADC measurement, and numerous prospective and retrospective investigations have supported this finding [24,25]. It was also shown to be significant that ADC measurement was added to the recently published ovarian-adnexal reporting and data system (O-RADS). ADC and whole lesion ADC histogram measurements have been shown to be useful in separating low-to-intermediate risk and intermediate-to-high risk adnexal masses, which may potentially change the clinical management of patients when planning surgery, when added to the O-RADS MRI score 4 [26].

Another study found that by incorporating the ADC mean values, the diagnostic efficacy of O-RADS MRI scoring for adnexal lesions characterization could be improved by decreasing false positives, increasing specificity, and preserving good sensitivity [27].

Our study has a number of drawbacks. First, because the study was retrospective in nature, a selection bias was unavoidably present. Second, there is no long-term follow-up of our patients following LRT, and this study is a single-center investigation on patients receiving various locoregional therapy. It is advised to do more extensive prospective investigations. The absence of pathological association is also regarded as a significant drawback of the study.

This is related to clinical practice, where a biopsy is not always necessary; nonetheless, our goal was to reduce the biopsy rates to be performed only for chosen cases that could not be resolved by imaging.

Conclusions:

Quantitative DWI analysis involving ROI ADC measurement could be beneficial if it is included in LI-RADS v2018 treatment response algorithm of HCC. When planning surgery, this might improve how patients are managed clinically. It is advised to standardize the DW MRI methodology and conduct prospective validation studies.

References

- PASCUAL S., HERRERA I. and IRURZUN J.: New advances in hepatocellular carcinoma. *World J. Hepatol.*, 8: 421-438, 2016.
- DREWES R., HEINZE C., PECH M., et al.: Apparent Diffusion Coefficient can Predict Therapy Response of Hepatocellular Carcinoma to Transcatheter Arterial Chemoembolization. *Dig. Dis.*, 40: 596-606, 2022.
- BRUIX J. and SHERMAN M.: Management of hepatocellular carcinoma: An update. *Hepatology*, 53: 1020-1022, 2011.
- CESCON M., CUCCHETTI A., RAVAIOLI, et al.: Hepatocellular carcinoma locoregional therapies for patients in the waiting list. Impact on transplantability and recurrence rate. *J. Hepatol.*, 58: 609-618, 2013.
- HEIMBACH J.K., KULIK L.M., FINN R., et al.: AASLD guidelines for the treatment of hepatocellular carcinoma. *Hepatology*, 67: 358-380, 2018.
- European Association for the Study of the Liver. EASL Clinical Practice Guidelines: Management of hepatocellular carcinoma. *J. Hepatol.*, 69: 182-236, 2018.
- RAZEK A.A.K.A., EL-SEROUGY L.G., SALEH G.A., et al.: Liver imaging reporting and data system version 2018: what radiologists need to know. *J. Comput Assist Tomogr.*, 44 (2): 168-77, 2020.
- ALLARD M.A., SEBAGH M., RUIZ A., et al.: Does pathological response after transarterial chemoembolization for hepatocellular carcinoma in cirrhotic patients with cirrhosis predict outcome after liver resection or transplantation? *J. Hepatol.*, 63: 83-92, 2015.
- PRAJAPATI H.J., SPIVEY J.R., HANISH S.I., et al.: mRECIST and EASL responses at early time point by contrast-enhanced dynamic MRI predict survival in patients with unresectable hepatocellular carcinoma (HCC) treated by doxorubicin drug-eluting beads transarterial chemoembolization (DEB TACE). *Ann. Oncol.*, 24: 965-673, 2013.
- KAMEL I.R., BLUEMKE D.A., RAMSEY D., et al.: Role of diffusion-weighted imaging in estimating tumor necrosis after chemoembolization of hepatocellular carcinoma. *AJR Am. J. Roentgenol.*, 181: 708-710, 2003.
- XU J., DOES M.D. and GORE J.C.: Sensitivity of MR diffusion measurements to variations in intracellular structure: Effects of nuclear size. *Magn. Reson. Med.*, 61: 828-833, 2009.
- HARKINS K.D., GALONS J.P., SECOMB T.W., et al.: Assessment of the effects of cellular tissue properties on ADC measurements by numerical simulation of water diffusion. *Magn. Reson. Med.*, 62: 1414-1422, 2009.
- YOUN S.Y., KIM D.H., CHOI S.H., et al.: Diagnostic performance of Liver Imaging Reporting and Data System treatment response algorithm: A systematic review and meta-analysis. *Eur. Radiol.*, 31: 4785-4793, 2021.
- RAZEK A.A., EL-SEROUGY L.G., SALEH G.A., et al.: Reproducibility of LI-RADS treatment response algorithm for hepatocellular carcinoma after locoregional therapy. *Diagn. Interv. Imaging*, 101 (9): 547-53, 2020.
- GERVAIS D.A.: LI-RADS treatment response algorithm: Performance and diagnostic accuracy. *Radiology*, 292: 235-236, 2019.
- American College of Radiology (ACR). Liver Imaging Reporting and Data System (LI-RADS) (2017). ACR website. <https://www.acr.org/Clinical-Resources/Reporting-and-Diagnostic-Systems/LI-RADS.published> . Accessed April 3, 2018.
- KOO T.K. and LI M.Y.: A guideline for selecting and reporting intraclass correlation coefficients for reliability research. *Journal of Chiropractic Medicine*, 15: 155-163, 2016.
- SCHRAML C., SCHWENZER N., CLASEN S., et al.: Navigator Respiratory-Triggered Diffusion-Weighted Imaging in the Follow-up after Hepatic Radiofrequency Ablation-Initial Results. *J. Magn. Reson Imaging*, 29: 1308-1316, 2009.
- MAHMOUD B.E., GADALLA A. AEH and ELKHOLY S.F.: The role of dynamic and diffusion MR imaging in therapeutic response assessment after microwave ablation of hepatocellular carcinoma using LI-RADS v2018 treatment response algorithm. *Egypt. J. Radiol. Nucl. Med.*, 52: 1-10, 2021.
- LIU Z., FAN J.M., HE C., et al.: Utility of diffusion weighted imaging with the quantitative apparent diffusion coefficient in diagnosing residual or recurrent hepatocellular carcinoma after transarterial chemoembolization: A meta-analysis. *Cancer Imaging*, 20: 3, 2020.
- DREWES R., HEINZE C., PECH M., et al.: Apparent diffusion coefficient can predict therapy response of hepatocellular carcinoma to transcatheter arterial chemoembolization. *Dig. Dis.*, 40: 596-606, 2022.
- YU, J.I., PARK H.C2, LIM D.H., et al.: The role of diffusion-weighted magnetic resonance imaging in the treatment response evaluation of hepatocellular carcinoma patients treated with radiation therapy. *Int. J. Radiat. Oncol. Biol. Phys.*, 89: 814-821, 2014.
- LO C.H., HUANG W.Y., HSIANG C.W., et al.: Prognostic Significance of Apparent Diffusion Coefficient in Hepatocellular Carcinoma Patients treated with Stereotactic Ablative Radiotherapy. *Sci. Rep.*, 9: 14157, 2019.

- 24- JORDAN E.J., FISKE C., ZAGORIA R., et al.: PI-RADS v2 and ADC values: Is there room for improvement? Abdom. Radiol., 43: 3109-3116, 2018.
- 25- COSTA D.N., XI Y., AZIZ M., et al.: Prospective Inclusion of Apparent Diffusion Coefficients in Multiparametric Prostate MRI Structured Reports: Discrimination of Clinically Insignificant and Significant Cancers. AJR Am. J. Roentgenol., 212: 109-116, 2019.
- 26- HOTTAT N.A., BADR D.A., VAN PACHTERBEKE C., et al.: Added value of quantitative analysis of diffusion-weighted imaging in Ovarian-Adnexal Reporting and Data System magnetic resonance imaging. J. Magn. Reson. Imaging, 56: 158-170, 2022.
- 27- HAMED E.M., FRERE R.A.F. and ZAID N.A.: Impact of Adding Mean Apparent Diffusion Coefficient (ADC-mean) Measurements to O-RADS MRI Scoring For Adnexal Lesions Characterization: A Combined O-RADS MRI/ADCmean Approach (2023). Acad. Radiol., 30: 300-311, 2023.

القيمة المضافة لقياس معامل الانتشار الظاهري في تقييم سرطان الخلايا الكبدية بعد العلاج الموضعي باستخدام خوارزمية الاستجابة للعلاج

هذه الدراسة تم إجراؤها على ١١٧ مريضاً لديهم أورام خبيثة بالكبد تلقوا علاجاً موضعياً للورم اما بالكي الحراري للورم او التزدد الحراري او حقن علاج كيميائي عن طريق القسطرة الشريانية. تم عمل فحص رنين مغناطيسي بالصبغة مع اضافته قياس معامل الانتشار الظاهر لكل ورم معالج. تم استبعاد ٧ أشخاص من البحث بسبب عدم جوده صور الرنين المغناطيسي. ضمنت المجموعة النهائية ١١٠ أفراداً (٩٢ رجلاً و ١٨ امرأة) بمتوسط عمر ٥٤ عاماً (٤٩-٦١ عاماً) و ١٢٦ آفة سرطان الكبد. قد تم علاج ١٢٦ سرطان الكبد ال ١٢٦ التي تم تضمينها إما بالتردد الحراري (٣٠.٢٪ : ١٢٦/٣٨) ، بالكي الحراري (١٢٦/٣٦ : ٢٨.٦٪) ، أو حقن علاج كيميائي عن طريق القسطرة الشريانية (١٢٦/٥٢ : ٤١.٢٪).

قام كل مراقب بفحص ١٢٦ من سرطانات الكبد المعالجة إجمالاً. ويبين الجدول ١ عدد ملاحظات الكبد التي قام بها كل من الراصدين ضمن كل فئة من فئات (LR-TR). ومع ذلك ، كان فحص قياسات معامل الانتشار الظاهري في تقييمي المراقبين مختلف فئات LR-TR هو التركيز الرئيسي لهذا التحقيق.

وفقاً لمتوسط قيم معامل الانتشار الظاهري لكلا المراقبين ، كان سرطان الخلايا الكبدية القابل للحياة 0.17 ± 1.026 و 0.18 ± 1.04 و كان HCC غير القابل للحياة 0.19 ± 1.47 و 0.19 ± 1.48 و كان $3-10 \times$ مم 2 / ثانية.

يمكن أن يكون تحليل خاصية الانتشار الكمي الذي يتضمن قياس عائد الاستثمار لمعامل الانتشار الظاهري مفيداً إذا تم تضمينه في خوارزمية استجابة علاج LI-RADS v ٢٠١٨ لسرطان الكبد. عند التخطيط للجراحة، قد يؤدي ذلك إلى تحسين كيفية إدارة المرضى سريريًا. ينصح بتوحيد منهجية التصوير بالرنين المغناطيسي خاصة الانتشار وإجراء دراسات التحقق من الصحة المستقبلية.